Science Journal of Clinical Medicine
2021; 10(2): 52-64
http://www.sciencepublishinggroup.com/j/sjcm
doi: 10.11648/j.sjcm.20211002.17
ISSN: 2327-2724 (Print); ISSN: 2327-2732 (Online)

Identification of Functional Gene Modules and Biomarkers of Apatinib Against Lung Adenocarcinoma Based on Weighted Gene Co-expression Network Ansalysis (WGCNA)

Zhang Yanli[1], Luo Shiqiong[1], Zhong Yixuan[1], Wu Guosong[2], Zhang Zhidong[1, *]

[1]Department of Pharmacy, The First Affiliated Hospital of Jinan University, Guangzhou, China

[2]Baiyun Branch of Nanfang Hospital, Southern Medical University, Guangzhou, China

Email address:

rellyzhang2012@sina.cn (Zhang Yanli), tzzd0608@jnu.edu.cn (Zhang Zhidong)

[*]Corresponding author

To cite this article:

Zhang Yanli, Luo Shiqiong, Zhong Yixuan, Wu Guosong, Zhang Zhidong. Identification of Functional Gene Modules and Biomarkers of Apatinib Against Lung Adenocarcinoma Based on Weighted Gene Co-expression Network Ansalysis (WGCNA). *Science Journal of Clinical Medicine*. Vol. 10, No. 2, 2021, pp. 52-64. doi: 10.11648/j.sjcm.20211002.17

Received: June 10, 2021; **Accepted**: June 19, 2021; **Published**: June 25, 2021

Abstract: Objective: Apatinib is a drug for the treatment of gastric cancer. In recent years, studies have found that it also has good efficacy in the treatment of lung adenocarcinoma, but its mechanism of action is still not clear. Therefore, this study uses bioinformatics and Experimental verification explores the mechanism of apatinib in the treatment of lung adenocarcinoma. To explore the potential biological targets of apatinib against lung adenocarcinoma based on weighted gene co-expression network analysis (WGCNA). Methods: The PharmMapper server was first used to reversely predict the potential targets of apatinib. Subsequently, it was combined with WGCNA to mine the GSE10072 data set in the GEO database of the National Center for Biotechnology Information (NCBI) to obtain the co-expressed gene module. Next, it was combined with apatinib Predict the target matching mapping to obtain the potential anti-lung adenocarcinoma target of apatinib. The STRING database was combined with Cytoscape software to visualize the protein interaction network of apatinib's potential anti-lung adenocarcinoma target protein and perform network topology analysis, as well as to obtain the core target from the network. Kaplan Meier plotter database was applied to analyze the relationship between key genes and the prognosis of patients with lung adenocarcinoma. Molecular docking technology was used for the potential of apatinib. Anti-lung adenocarcinoma target protein was finally verified by molecular interaction. Finally, Western blot was employed to analyze the expression level of the key target protein. Results: A total of 300 targets of apatinib were obtained, and 45 potential targets of apatinib against lung adenocarcinoma were screened. From the protein interaction network analysis, the key genes included CASP3, EGFR, MMP9, SRC, CASP8, CASP9, STAT3 and MAPK1. High expression of EGFR, SRC, MAPK1 and STAT3, and low expression of CASP3, CASP8, CASP9 and MMP9 were closely related to poor prognosis of patients with lung adenocarcinoma. Molecular docking showed that the interaction of apatinib with the targets of MAPK1, CASP3, EGFR, SRC, MMP9 and STAT3 was comparable to the positive control. Western blot showed that with the increasing of drug concentration, STAT3 were down-regulated, and CASP8 were up-regulated. Conclusion: The mechanism of apatinib in the treatment of lung adenocarcinoma is mainly through the regulation of the signal transduction pathway and the apoptosis pathway, which provides a scientific basis for the study of its anti-lung adenocarcinoma mechanism.

Keywords: Bioinformatics, Apatinib, Lung Adenocarcinoma, Biomarker, Molecular Docking

1. Introduction

The incidence rate of lung cancer is increasing gradually. Every year, more than 5 million new lung cancer cases are diagnosed, with nearly ten thousand deaths [1]. Currently, lung cancer ranks first in the incidence and mortality of malignant tumors, seriously threatening human health and life. Non small cell lung cancer (NSCLC) is one of the most common lung cancer in clinical practice, accounting for about 85% of patients. The most common pathological type

is lung adenocarcinoma [2-3]. Patients with this tumor have no obvious symptoms in the early stage, and their condition is difficult to detect. Generally, it has already been in middle and late stage when first diagnosed, with a relatively low 5-year survival rate [4]. At present, platinum based dual drug chemotherapy is commonly used in the treatment of advanced NSCLC. However, it is easily to be drug-resistant, accompanied by many side effects and poor curative effect [5]. It is urgent to explore better drugs and schemes for NSCLC treatment, so as to improve the life quality and prolong the survival period of patients as much as possible. Smoking is an important factor in the occurrence and development of lung cancer. This leads to C → A base transversion and epigenetic changes in smokers, eventually making normal cells cancerous [6-7]. However, the potential therapeutic molecular targets and mechanisms of cigarette smoking still need to be further elucidated. Moreover, for the treatment of lung adenocarcinoma, traditional treatment strategies including surgery, radiotherapy and chemotherapy fail to obtain satisfactory significant survival benefits, and the overall survival rate of patients is low [8]. Therefore, further development of new drugs with the effect of non-small cell lung cancer has important clinical significance. In the future, this may provide the basis of drug selection and molecular target information for early diagnosis and treatment of lung cancer.

Apatinib is an innovative new drug independently developed in China. It is also the first anti-cancer drug that has been proved to be safe and effective in the treatment of advanced gastric cancer [9]. Apart from being used in the treatment of advanced gastric cancer, apatinib has shown good clinical efficacy in breast cancer [10], colorectal cancer [11] and non-small cell lung cancer [12]. A number of studies [13-16] have confirmed that apatinib has excellent therapeutic effect in advanced NSCLC. It can not only prolong the progression free survival of patients with ineffective chemotherapy, but also reduce the resistance of cancer cells to chemotherapy. Especially in the treatment of advanced lung adenocarcinoma, adverse reactions should be more predictable, tolerable and controllable, with significant curative effect and better safety. However, up to now, most of the researches mainly focus on the efficacy test single therapeutic target of apatinib in the treatment of lung adenocarcinoma. The specific overall mechanism is still unclear, which is not conducive to the development of new indications for apatinib and the elaboration of the mechanism for lung adenocarcinoma treatment.

Weighted correlation network analysis (WGCNA) is a system biology method that can mine module information from high-throughput data and describe gene association patterns between different samples. If a set of genes have similar expression changes in physiological processes or different tissues, WGCNA can mine module information from high-throughput data. Then these genes are related to function to a certain extent, and are defined as a modules [17]. Candidate biomarkers or therapeutic targets are identified according to the interconnection of modules and the association between modules and phenotypes. Kuang Haofa et al [18], Qi et al [19], An et al [20] used WGCNA to mine the pivotal genes in the occurrence and development of prostate cancer, non-small cell lung cancer, lung adenocarcinoma and other malignancies. They have found the core targets affecting the cancer process, which provides valuable theoretical information for promoting the understanding of human cancer. Therefore, WGCNA is widely used for screening disease marker or gene targets. It is also suitable for drug combination with high-throughput data to screen drug therapy targets and the mechanism of intervention in disease network.

In this study, we analyzed the differentially expressed genes in the data set downloaded from the geo database in NCBI, and used WGCNA to mine the differentially expressed genes related to smoking history. We also intersected with drug prediction targets, and screened out the core targets of apatinib in the treatment of lung adenocarcinoma. The Kaplan Meier plotter database was used to preliminarily explore the clinical significance of core targets in lung adenocarcinoma. Finally, the interaction between drugs and their core targets was verified by molecular docking technology. All these findings might help to provide a reference for further study on the mechanism of apatinib in the treatment of lung adenocarcinoma.

2. Method

2.1. Bioinformatics Method

2.1.1. Prediction of Target of Apatinib

The 3D structure of apatinib was obtained from PubChem (https://www.ncbi.nlm.nih.gov/pccompound/) and saved in SDF format. PharmMapper Server (htte:/iab.ecust.lcdu.cn Pharmmapper/) is an open source and large-scale web server with more than 7000 receptor based pharmacophore models (covering 1627 drug target information, 459 of which are human protein targets). It aims to identify potential candidate targets of small molecule drugs with given probes by using pharmacophore mapping method. The pure fitting scores obtained by this method have high statistical significance and reliability. In this study, the SDF format of apatinib was input into pharmmapper sever for reverse docking, and the first 300 targets for screening human sources were set. By default, the remaining parameters remained unchanged.

2.1.2. Clinical Data Sources of Lung Adenocarcinoma

GEO database, full name of gene expression omnibus, is a gene expression database created by National Biotechnology Information Center (NCBI) of the United States. It contains high-throughput gene expression data submitted by research institutions all over the world [21]. In order to further explore the clinical significance of apatinib as a predictive target, we used the keyword "lung adenocarcinoma" in the GEO datasets of NCBI in this study, and selected the data set with pathological control samples larger than 15 cases. GSE10072 transcriptome chip was used to detect the whole genome gene data set, which contained 89 samples

(including 58 tumor samples and 31 normal control non tumor samples). GEO2R analysis tool in GEO database was used to normalize the original strength data of chips, and box diagram visualization was used to analyze the reliability of data. Clinical information included gender, age and smoking history.

2.1.3. Identification of Core Targets of Components Related to Genes of WGCNA Coexpression Module and Clinical Information Module

Limma package (version: 3.40.2) of R software was used to study the differential expression of mRNAs. The adjusted P-value was analyzed to correct for false positive results in GSE10072. "Adjusted $P < 0.05$ and Log (Fold Change) > 1 or Log (Fold Change) < −1" was defined as the threshold for the screening of differential expression of mRNAs. The WGCNA package of R software was used to study the correlation patterns among all differentially expressed genes of GSE10072. Gene modules related to clinical information were obtained. The Pearson correlation coefficient of each gene was calculated, and weighted adjacency matrix $aMn = |C\ Mn|\ \beta$ was constructed, where a Mn was the adjacent coefficient of gene m and gene N; C Mn was the Pearson correlation coefficient of gene m and gene n. Soft threshold value $\beta = 9$ was selected to ensure the construction of scale-free network. The deepspplit value was 2 and the minimum module size was 30. Three genes were identified to generate a dendrogram. The highly similar modules were identified by clustering, and the similar modules were merged with the high shear critical value of 0.25. In addition, Pearson correlation analysis was used to calculate the correlation coefficient and P value between characteristic genes of the gene module and the external clinical information, and were vividly displayed in the form of heat map by labeled Heatmap function. The most relevant gene modules and clinical features were selected as research objects, so as to find the gene modules with biological significance.

2.1.4. PPI Network Construction and Hub Gene Recognition

The prediction target of apatinib and smoking history were identified by venny diagram, and their common genes against lung adenocarcinoma were obtained. In order to further explore the possible synergistic effect of the common target genes of apatinib, we used the string database (https://string-db.org/Version 10.5) construct target PPI network in this study. The network was imported into Cytoscape (version 3.6.1, http://www.cytoscape.org). Visual analysis was carried out, and the network topology was calculated by using the network analyzer analysis module to meet the node degree value (degree). When DG was greater than two times of DG, one time of closeness (CC) and one time of betweenness (BC), the larger the values of these three values, it might play an important role in maintaining the overall structure of the network [22-23].

2.1.5. Clinical Prognostic Value of Core Target

Kaplan Meier plotter (http://kmplot.com/analysis/index.php?p=background) database was used to analyze the overall survival rate of patients, so as to evaluate the prognostic value of hub targets.

2.1.6. Molecular Docking Verification

Molecular docking can simulate the interaction between receptors and ligands by chemometrics to accurately predict the possibility of their binding. It can also optimize the structure of receptors and ligands according to their binding conditions [24]. The target points were obtained from the PDB database (http://www.rcsb.org/pdb) using discovery studio 2.5 and autodock 1.5.6, PyMOL and other visualization and simulation software, to deal with drugs and targets, as well as to explore the binding situation of the two from the molecular level. At present, most drugs compete with endogenous ligands of receptor molecules and interfere with their active sites. Therefore, the binding free energy and binding bond of the ligand with crystal structure of the target could be used a reference to accurately understand the interaction between targets and active small molecules.

2.2. Experimental Evidence

2.2.1. Cells and Main Equipment

Human lung adenocarcinoma A549 cell (337696, BeiNa Chuanglian Biotechnology Co., Ltd.). Apatinib standard was purchased from Selleck. CASP8 and STAT3 antibodies were purchased from Abcam. BCA protein quantification kit (A00755), SDS-PAGE gel preparation kit (50426) and RIPA lysate (R0020) were all purchased from Beijing Kangwei Century Biotechnology Co., Ltd. RPMI-1640 medium and fetal bovine serum were purchased from GIBCO Company. Trypsin was purchased from Bioind. Dimethyl sulfoxide (DMSO) was purchased from Biyuntian Company. Inverted microscope (AE2000, Olympus Co., Ltd., Japan); multifunctional fluorescence imager (Odyssey CLX, Licor, USA).

2.2.2. Grouping and Administration

Lung adenocarcinoma A549 cells suspension in the logarithmic growth phase was uniformly inoculated into a 6-well plate and divided into blank control group, Apatinib 8 μM administration group, Apatinib 16 μM administration group, and Apatinib 32 μM administration group. When the cell confluence rate was from 70% to 80%, different concentrations of Apatinib were added to the administration group. Meanwhile, culture medium was added to the control group, and the protein was extracted 24 hours later. Each experiment was repeated 3 times independently, and the average value was taken as well.

2.2.3. Western Blot (WB) Detecting the Expression Level of Related Proteins

The extracted total protein of each group of cells was collected, and the protein concentration was determined by adopting BCA method. After gel electrophoresis transfer membrane, and the corresponding primary antibody and secondary antibody were incubated. ImageJ software was used to analyze the gray value of each band after development

and the gray value of the internal reference GAPDH. At the same time, the degree value ratio is used for statistical analysis.

2.2.4. Statistical Processing

SPSS20.0 software was applied for statistical analysis, and GraphPad Prism version 5.01 software was used for data analysis and graphing. The two-sample mean t test was carried out for comparison among groups in the experiment, and $P<0.05$ was considered statistically significant.

3. Results

3.1. Construction of Weighted Co Expression Network and Determination of Hub Module

As shown in Figure 1, after normalization of the original signal intensity data of 58 tumor samples and 31 normal control non tumor samples, the median values were relatively in the same horizontal line, indicating that the selected samples were reasonable and comparable. In this study, $\beta = 9$ ($R^2 = 0.89$) was selected as the soft threshold (Figure 2-A). The linkage among genes in the network conformed to the scale-free network distribution, and the results were shown in Figure 2-b. The results of differential analysis showed that compared with normal group (Figure 3-4), 2541 mRNAs were differentially expressed in tumor group, including 1576 up-regulated and 965 down-regulated. Dynamic tree-cutting can identify modules, and gene expression values in the modules are similar. Highly similar modules were combined. A total of 8 co-expressive modules were identified, with the size of 22-1841 genes. Each module was labeled with one color (Figure 5-A). In the module feature relationship diagram (Figure 5-B), the green ($r = 0.22$, $P = 0.02$) module and red ($r = 0.2$, $P = 0.04$) modulehad a significant positive correlation with the characteristics of patients' smoking history. Therefore, in the subsequent analysis, green, red modules and smoking history were taken as clinical features to be studied.

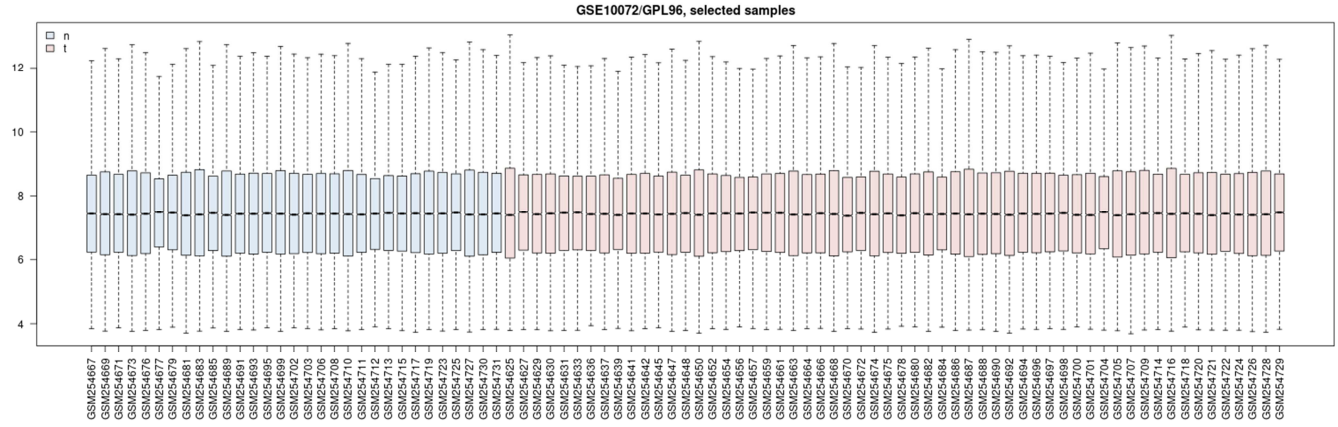

Pink represents control samples; light blue represents tumour samples.

Figure 1. *Normalized value distribution of sample original strength.*

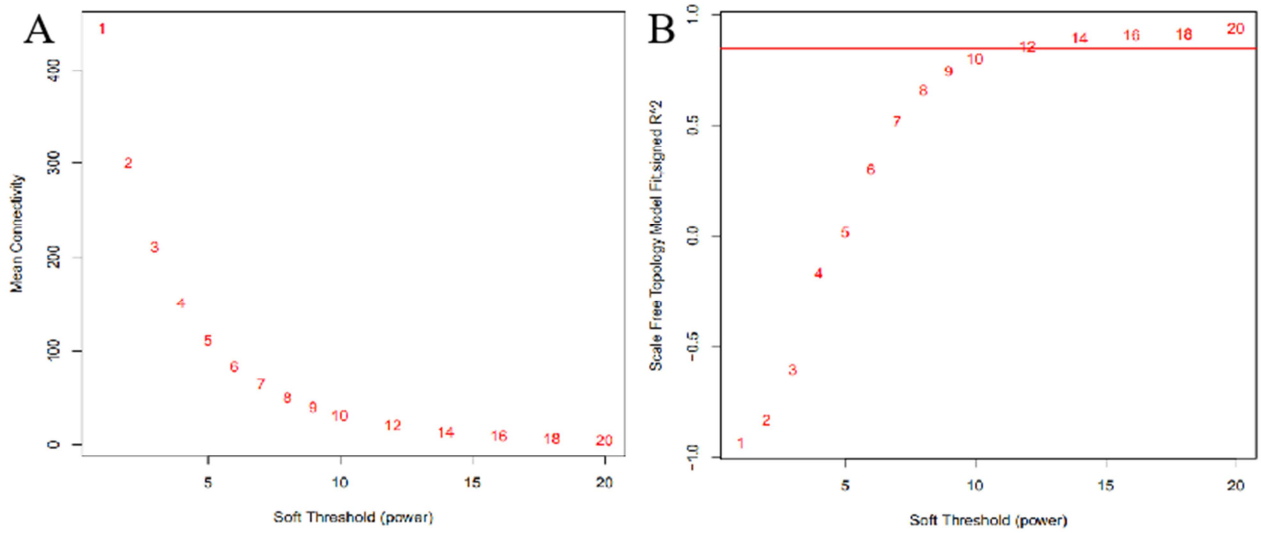

Figure 2. *Analysis of network topology with soft threshold parameters.*

A. Scale-free fitting index (Y-axis) as a function of soft threshold parameter (x-axis).
B. Average connectivity (Y-axis) as a function of soft threshold parameter (x-axis).

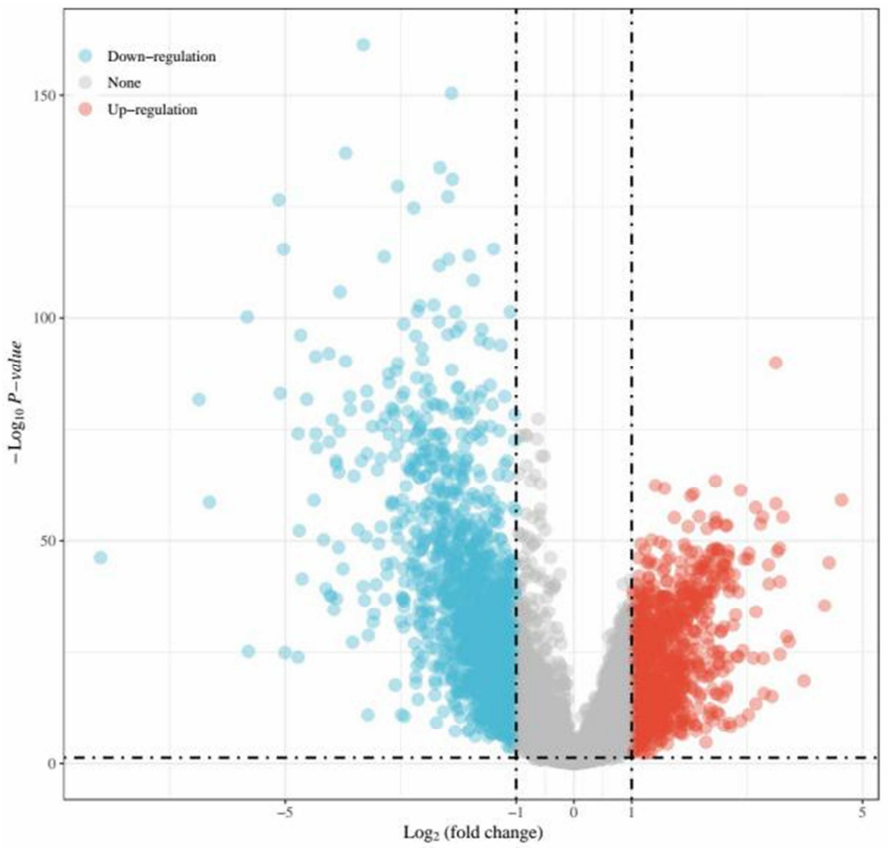

Figure 3. *Volcanic map.*

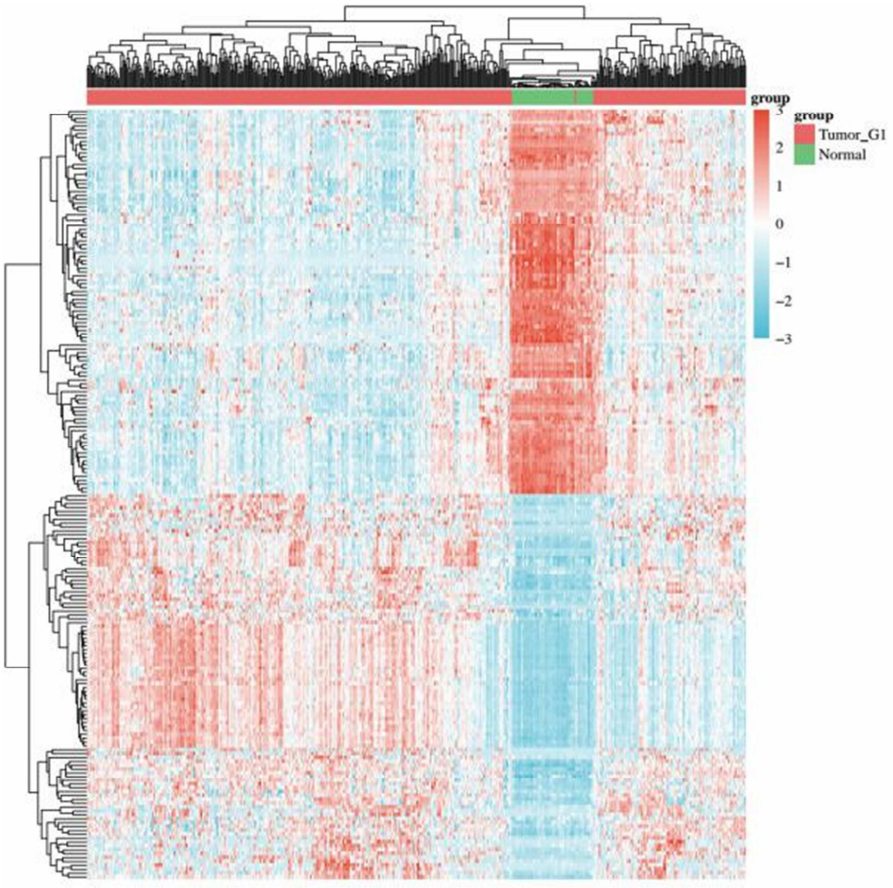

Figure 4. *Differential gene expression heatmap.*

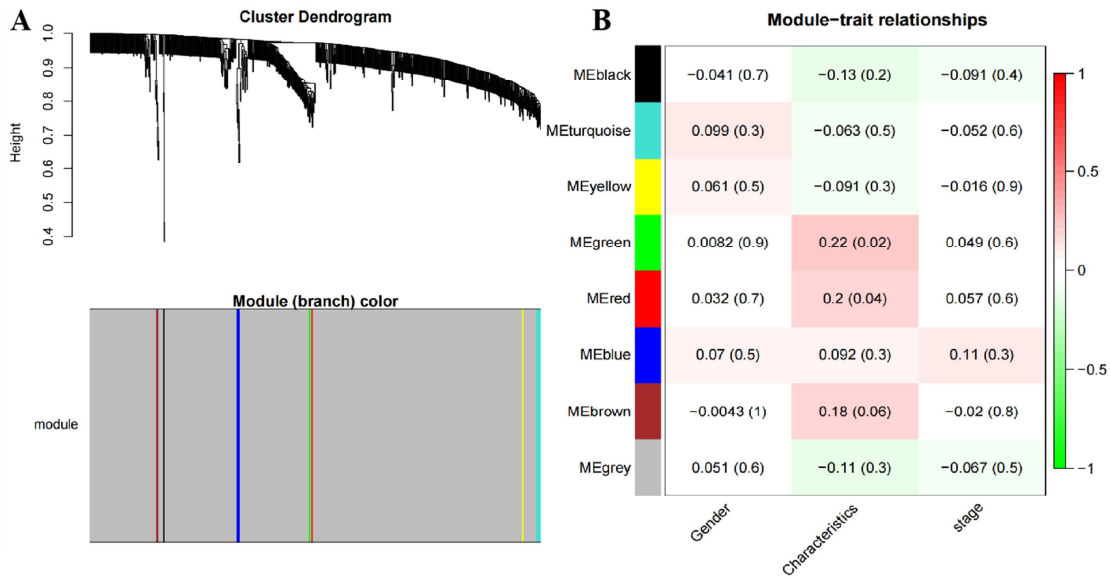

Figure 5. *Determination of clinical features of gene association in modules.*

A-gene clustering tree obtained by hierarchical of adjacency-based dissimilarity. B-relationship of module and feature. Each row represents a module eigengene and each column to a clinical feature. Each rectangle contains the corresponding correlation in the first line and the *P*-value in the second line. The table uses color to indicate the significance of the correlation.

3.2. Determination of Core Anticancer Targets of Apatinib

The target genes corresponding to apatinib were matched with those related to red and green modules to obtain common genes, which were the potential targets of apatinib against lung adenocarcinoma. As shown in Figure 6, a total of 45 apatinib potential anti-lung adenocarcinoma genes were identified, of which 45 targets were from the communication part of apatinib and red plate, and 5 targets were from the matching of apatinib and green plate. The median values of DG, CC and BC of the network were 12, 0.57 and 0.0041, respectively, which met the topological parameter threshold of this study. As shown in Figures 7-9, MAPK1 (DG =36, CC = 0.810, BC = 0.129), STAT3 (DG = 34, CC = 0.783, BC = 0.055), SRC (DG = 34, CC = 0.783, BC = 0.086), CASP3 (DG = 32, CC = 0.758, BC = 0.037), EGFR (DG = 31, CC = 0.746, BC = 0.088), MMP9 (DG = 28, CC = 0.701, BC = 0.067), CASP9 (DG = 25, CC = 0.635, BC = 0.007), and CASP8 (DG = 25, CC = 0.627, BC = 0.048) were potential core targets of apatinib against lung adenocarcinoma.

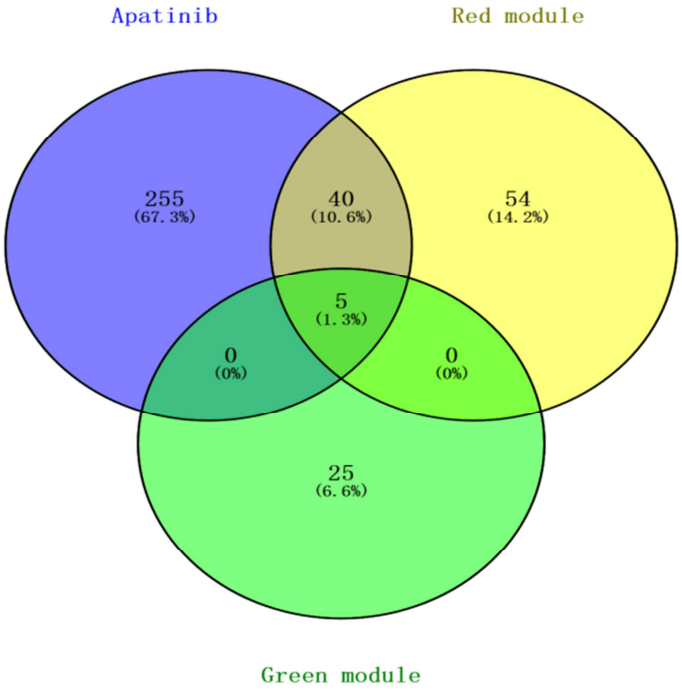

Figure 6. *Venn graph.*

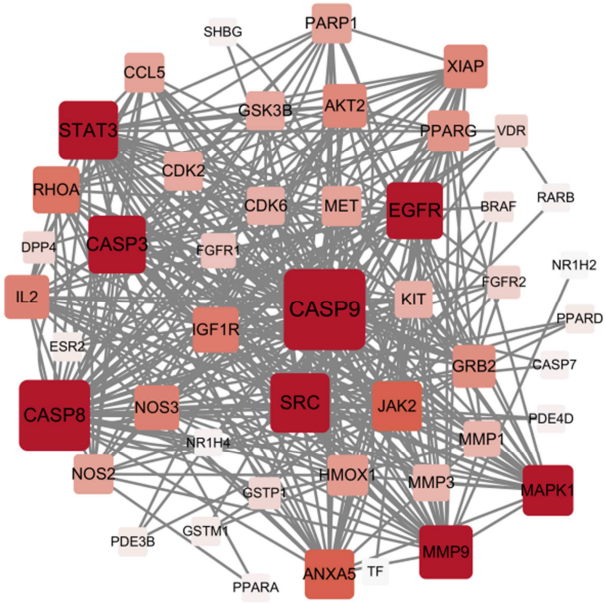

Figure 7. *Intervention target.*

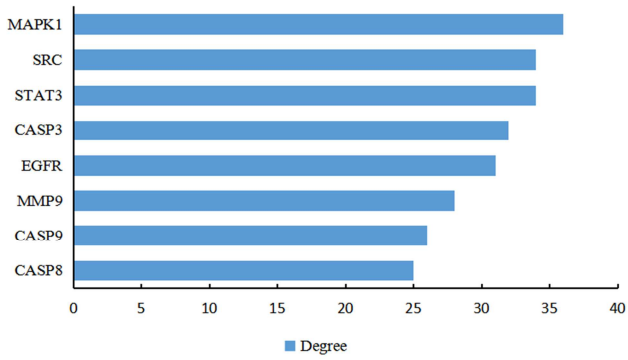

Figure 8. *Topological parameters of key targets.*

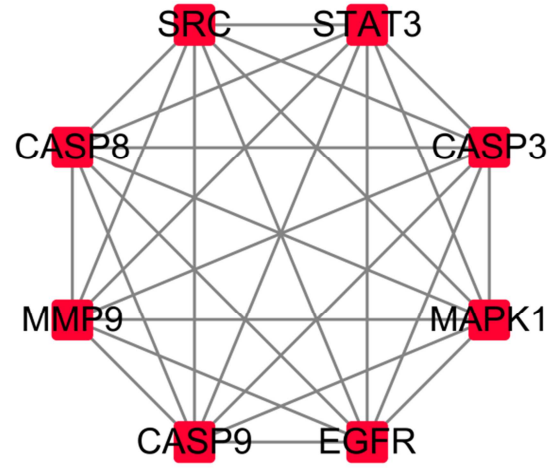

Figure 9. *Key target network diagram.*

3.3. Clinical Significance of Key Targets of Apatinib

In order to further explore the clinical significance of the identified potential anticancer targets of apatinib, the impact of abnormal expression targets on the survival rate of patients was investigated by Kaplan Meier plotter database. Therefore, we might to evaluate the therapeutic and prognostic value of key targets. According to the overall survival rate analysis of target genes, high expression of MMP9 (HR = 1.14, lgP = 0.046), SRC (HR=1.21, lgP=0.0025), MAPK1 (HR=1.26, lgP=2.8×10-8), STAT3 (HR=1.64, lgP=0.02) was significantly associated with poor survival and prognosis. Low expression of CASP3 (HR = 0.85, lgP = 0.013), CASP8 (HR = 0.74, lgP = 3.6×10-6), CASP9 (HR = 0.75, lgP = 5.5×10-7) and EGFR (HR = 0.82, lgP = 0.021) was remarkably associated with poor survival and prognosis. The results were shown in Figure 10.

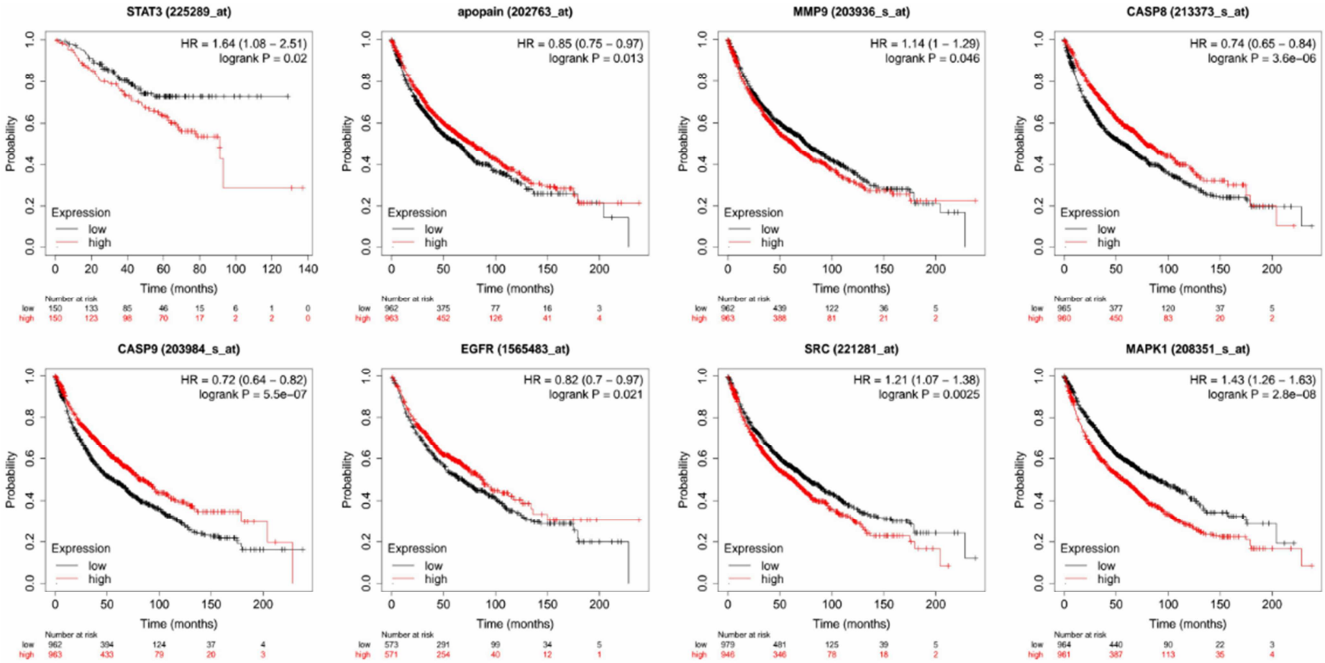

Figure 10. *Effect of key target of apatinib on the overall survival of lung adenocarcinoma.*

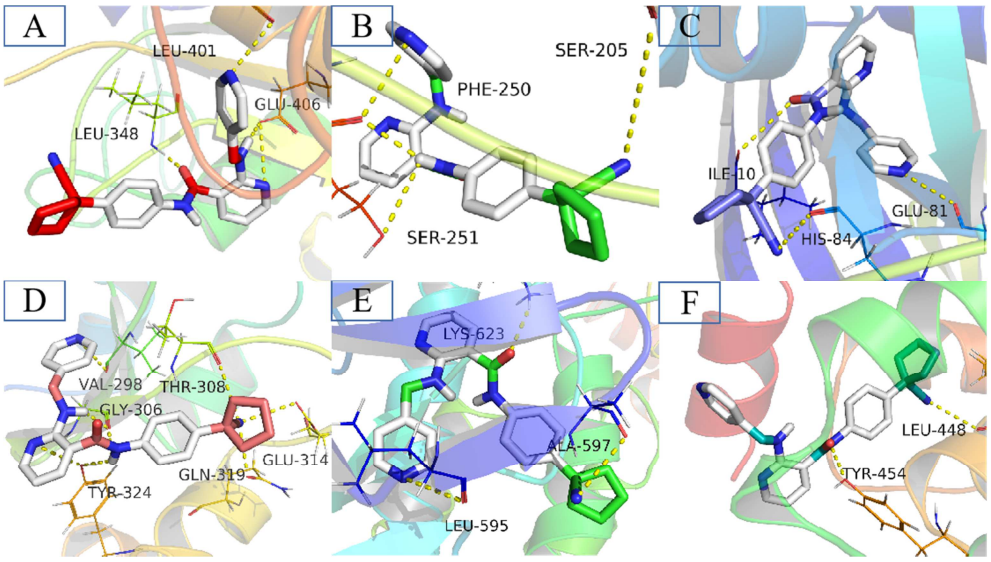

Figure 11. *Docking results of apatinib with CASP3 (A), EGFR (B), SRC (C), MAPK1 (D), MMP9 (E), STAT3 (F).*

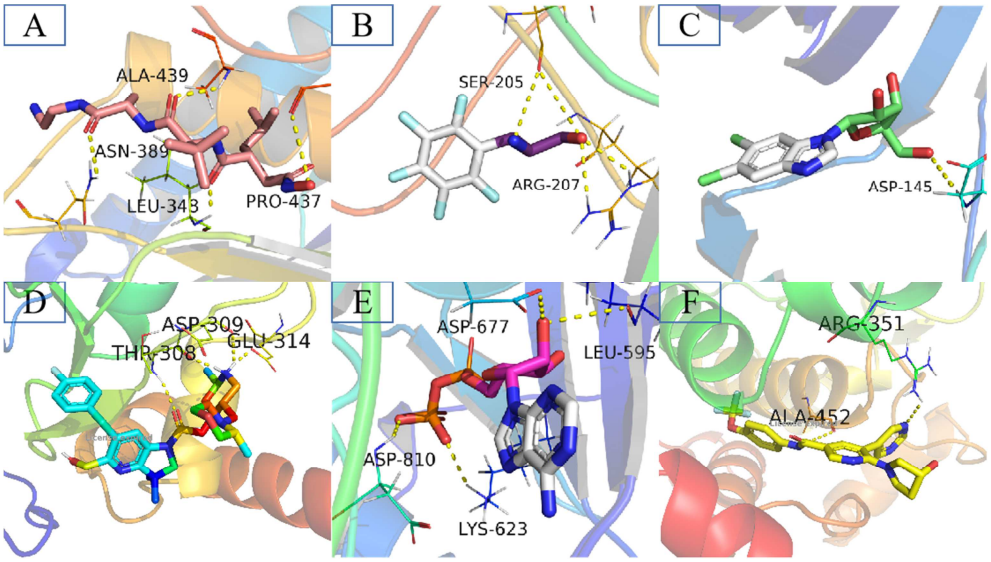

Figure 12. *Docking results of CASP3 (A), EGFR (B), SRC (C), MAPK1 (D), MMP9 (E), STAT3 (F) with their ligands.*

3.4. Molecular Docking Verification

In recent years, computer virtual screening technology has been used to screen disease targets for drug therapy. This helps to screen out possible drug targets from large databases and reduce the experimental cost to the greatest extent [25]. Autodock is an open-source molecular docking software that is widely used in X-ray crystallography, drug structure design, therapeutic target screening, chemical mechanism and other research. It can help us to clearly and accurately analyze the interaction between targets and active molecules [26]. Therefore, the docking of apatinib with MAPK1, CASP3, EGFR, SRC, MMP9 and other eight proteins was analyzed by autodock software in this study. The results found that apatinib had different degrees of binding with these eight targets (see Table 1). The binding free energy of apatinib with SRC, EGFR, MAPK1, CASP3, MMP9 and STAT3 was better than that of the original ligand. However, there were hydrogen bonds between apatinib and IEU-401, LEU-348 and GLU-406 of CASP3 (Figure 11A); there were hydrogen bonds between apatinib and PHE-250, SER-251 and SER-205 of EGFR (Figure 11B); there were hydrogen bonds between apatinib and GLU-81, HIS-84 and ILE-10 of SRC (Figure 11C); there were hydrogen bonds between apatinib and VAL-298, THR-308, GLY-306, TYR-324, GLN-319 and GLU-314 of MAPK1 (Figure 11D); there were hydrogen bonds between apatinib and LYS-623, ALA-597 and LEU-595 of MMP9 (Figure 11E); there were hydrogen bonds between apatinib and TVR-454 and LEU-488 of STAT3 (Figure 11F). These results indicated that there was a stable interaction between apatinib and eight predicted targets, among which the binding with MAPK1, CASP3, EGFR, SRC, MMP9 and STAT3 was the best. The above findings suggested that these targets were important potential targets of apatinib in the treatment of lung adenocarcinoma. The molecular docking of targets and its original ligands. (Figure 12)

Table 1. *Results of molecular docking.*

Target name	Binding freeenergy/kcal/mol		Target name	Binding freeenergy/kcal/mol	
	Apatinib	Original ligand		Apatinib	Original ligand
CASP3 (3HOE)	-8.6	-8.3 (HOE)	CASP8 (3H11)	-8.5	-9.7 (ASA)
EGFR (4LRM)	-8.7	-8.6 (YUN)	CASP9 (2AR9)	-8.5	-8.7 (MLT)
SRC (4U5J)	-8.7	-7.0 (RXT)	MMP9 (6ESM)	-9.9	-9.8 (BE4)
MAPK1 (5LCJ)	-10.4	-8.2 (6TS)	STAT3 (4ZIA)	-8.7	-7.8 (FMT)

3.5. Experimental Evidence

Some studies [27] have confirmed that apatinib can inhibit the proliferation, migration and invasion of lung adenocarcinoma cells by downregulating MMP9, MMP2 and other matrix metalloproteinase related proteins. Some studies [28] have found that the serum levels of MMP9 and other proteins in apatinib-treated NSCLC patients are significantly reduced. The corresponding treatment effective rate of this group is 97.67, which is higher than that of the control group 83.72% of paclitaxel combined with cisplatin. EGFR is one of the therapeutic targets of NSCLC, and the main first-line treatment drugs include Gefitinib, Erlotinib and other EGFR-TKI. However, most patients will develop drug resistance within about one year [29]. Li et al.[30] have conducted a retrospective study and found 16 patients with NSCLC choose to continue receiving eg after the first-line treatment with gefitinib, erlotinib or icotinib fails. The results of EGFR-TKIi and combined with apatinib showed that 4 patients still achieved partial remission (PR) and 10 stable patients (SD) among the 14 evaluable patients, with a median PFS of 4.6 months. In addition, there are some small-sample single-center retrospective studies and clinical case reports showing that apatinib combined with EGFR-TKI has a good effect in the treatment of NSCLC patients with EGFR mutation [31]. A number of prospective clinical trials of apatinib combined with EGFR-TKI are still under way. Lin et al. [32] have found that apatinib can significantly inhibit the growth, invasion and metastasis of human lung adenocarcinoma A549 cells transfected with KIF5B-RET. The possible underlying mechanism is to achieve the metastasis and invasion ability of KIF5B-RET positive tumor by inhibiting the phosphorylation of RET and SRC. As a downstream signal of KIF5B-RET pathway, SRC is the main protein that mediates cell invasion and metastasis. It is inhibited at the same time with RET phosphorylation, suggesting that apatinib has a dual inhibitory function on the development of human lung adenocarcinoma A549 cells and plays a dual anti-cancer role. In addition, other studies have found that the proliferation rate of lung adenocarcinoma H1650 cells treated with apatinib is significantly reduced. However, the apoptosis rate increases significantly, which may be achieved by upregulating CASP3 and other proteins to promote cancer cell apoptosis [33]. Apatinib can promote the apoptosis of lung adenocarcinoma in a dose-dependent manner through upregulating CASP3, CASP9 and Bcl2-Bax, downregulating Bcl-2, and inhibiting the activity of the ERK signaling pathway [34].

According to the above studies, although there is no report about the effect of apatinib on the progression of lung adenocarcinoma by regulating the targets of CASP8 and STAT3, the present study found that low expression of CASP8 and high expression of STAT3 were closely related to poor prognosis of lung adenocarcinoma patients by using public database mining. The molecular docking results showed that apatinib had a good combination with both. Some studies have confirmed that apatinib can regulate the apoptotic pathway with protein core such as CASP3, CASP9 and BCL2-Bax / Bak. Does it also regulate Fas pathway to induce apoptosis? The activity of CASP8 protein can be detected in the later stage. STAT3 is the downstream target of ERK and SRC. When the activity or expression of ERK and SRC is inhibited by apatinib, STAT3 will also be inhibited theoretically. However, this needs further experimental verification.

As shown in Figure 13, after treating A549 cells with different concentrations of Apatinib for 24 hours, the protein expression was detected by WB. It was obvious that, with the increase of drug concentration, the expression of STAT3 was significantly down-regulated, and the expression of CASP8 was remarkably up-regulated, with statistically significant differences ($P < 0.05$). It is suggested that Apatinib can also interfere with the apoptosis and signal transduction process of lung adenocarcinoma by regulating CASP8 and STAT3, thereby inhibiting the growth and development of lung adenocarcinoma cells.

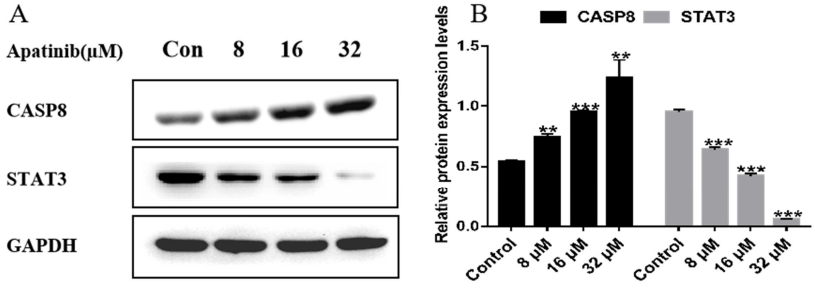

Compared with Con group, *P<0.05.

Figure 13. *Effects of Apatinib on protein expression (A-B) of A549 cells.*

In conclusion, the mechanism of apatinib in the treatment of lung adenocarcinoma is mainly through the regulation of the signal transduction pathway and the apoptosis pathway, as shown in Figure 14.

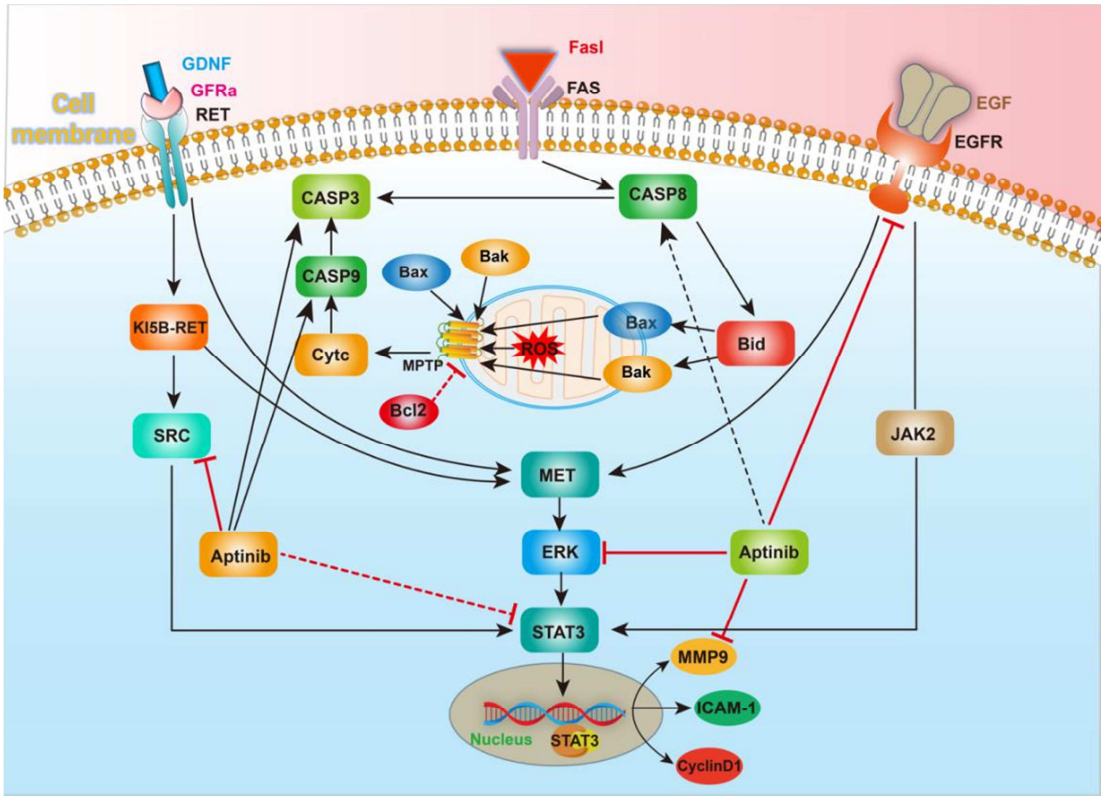

Figure 14. *Mechanism of apatinib in the treatment of lung adenocarcinoma.*

4. Conclusion

Lung cancer is one of the malignant tumors with highest mortality rate in the world. The development of safe and effective new treatment methods and identification of target information related to early diagnosis, treatment and prognosis of lung cancer are important issues to be improved in the current clinical treatment of lung cancer.

In this study, WGCNA was used to explore potential targets related to clinical prognosis. Finally, 300 targets were predicted by using PharMmapper. Meanwhile, WGCNA method was used to analyze GSE10072 data set in GEO database, and gene co-expression modules closely related to smoking history were obtained. Through mapping and matching with prediction targets of apatinib, 45 potential anti-lung adenocarcinoma targets of apatinib were identified.

According to the analysis of protein-protein interaction network of apatinib potential anti-lung adenocarcinoma targets, CASP3, EGFR, MMP9, SRC, STAT3, MAPK1, CASP8, CASP9 may have a good binding with apatinib and clinical significance. It has been reported [35] that epidermal growth factor receptor (EGFR) is one of the members of epidermal growth factor receptor family and is a transmembrane glycoprotein. It usually exists on the surface of epithelial cells and is overexpressed in malignant tumors. The EGFR signaling pathway plays an important role in the occurrence and development of lung cancer. EGFR often has deletion mutation in amino acid residues 747 to 750 in exon 19 and L858R point mutation in exon 21. Mutant EGFR promotes autophosphorylation of tumor cell receptor and activation of tyrosine kinase, eventually affecting the proliferation, metastasis, invasion and angiogenesis of tumor cells [36]. CASP3, CASP8 and CASP9 proteins, as the main members of the CASP family, can produce a cascade effect after being activated. CASP3 is one of the most important executive factors in the apoptosis pathway. High expression of CASP3 promotes the apoptosis of tumor cells, thus inhibiting the growth of tumor cells [37]. The abnormal expression of CASP3 is closely related to a variety of cancers [38-41]. Some studies have found that CASP3 may play an important role in the occurrence and development of lung adenocarcinoma [42-44]. It is reported more than 90% of cancer patients die of cancer cell metastasis and invasion [45]. As the protective barrier of microenvironment, basement membrane and extracellular matrix can effectively prevent the proliferation of cancer cells. When the defense line is penetrated by proteolysis, tumor cells can start the biological process of cell metastasis through cascade effect. Therefore, the invasion of cancer cells benefits from the degradation of extracellular matrix [46]. The matrix metalloproteinases of extracellular matrix mainly include MMP2, MMP3, MMP9, etc. It can be seen that MMP9 is closely related to the progression of cancer patients. Some other studies have confirmed that there is a significant difference in the

expression of MMP9 in lung adenocarcinoma [47]. In addition, SRC tyrosine kinase is closely related to tumor cell growth, metastasis, cell signal transduction and angiogenesis. This target has been recognized as an important anti-tumor target [48], and is also a research hotspot of tumor treatment [49, 50]. Previous studies [51-53] have confirmed that Src kinase inhibitor PP2 can inhibit the proliferation, migration and invasion of lung cancer cells by inhibiting the activity of the enzyme. Extracellular signal regulated kinase (ERK, MAPK1) is a mitogen activated protein kinase and an important member of the MAPK family [54]. It can transmit various extracellular stimulus signals to the nucleus through a series of cascade reactions. ERK promotes the phosphorylation of various transcription factors in the nucleus, and enhances the transcriptional activity, thus regulating tumorigenesis, proliferation and apoptosis [55]. ERK is overexpressed in many human cancers [56], such as oral cancer, melanoma, breast cancer, lung cancer, etc. STAT3, a nuclear transcription factor, is the intersection of many oncogenic cytokine signal transduction pathways. It participates in the regulation of multiple tumor related signal pathways, including proliferation, apoptosis, invasion and metastasis of malignant tumor cells, as well as immune escape [57]. Its signal transduction pathways exist in breast cancer, head and neck squamous cell carcinoma, lung cancer, pancreatic cancer, gastric cancer, and cervical squamous cell carcinoma. It is highly expressed in a variety of malignant tumors, such as ovarian cancer and colorectal cancer. Studies [58] have found that there are four pathways in the STAT3 signal transduction pathway, one of which is MAPK pathway activated by receptor tyrosine kinase (RTK). It has been found involved in the regulation of a large number of oncogenes and tumor suppressor genes. These targets are closely related to the occurrence and development of lung adenocarcinoma, serving as important genes in the process of lung adenocarcinoma deterioration as well. Therefore, the intervention of these targets may be the key to the treatment of lung adenocarcinoma with apatinib.

In this study, we analyzed and discussed the predicted target of apatinib and anti-lung adenocarcinoma. The results were consistent with the results reported in the literature, indicating that the combination of bioinformatics and target prediction had certain reliability in clinical data mining strategy. This study preliminarily revealed the characteristics of apatinib anti-lung adenocarcinoma targets, and provided a reference for further study of potential targets with good binding capacity with apatinib. In conclusion, the mechanism of apatinib in the treatment of lung adenocarcinoma is mainly through the regulation of the signal transduction pathway and the apoptosis pathway.

References

[1] Chen, W. Q., Li, N., Shi, J. F. (2019). Progress of Cancer Screening Program in Urban China. China Cancer, 28 (01): 1-11.

[2] Zheng, Y. Z., Ma, R., Zhou, J. K. (2016). ROR1 is a novel prognostic biomarker in patients with lung adenocarcinoma. Scientific Reports, 6, 36447.

[3] Siegel, R., Naishadham, D., Jemal, A. (2013). Cancer statistics, 2013 O-CA Cancer. Cin, 63 (1): 1-30.

[4] Pan, C. X. (2019). Progress in targeted treatment of non-small cell lung cancer. Internal Medicine, 014 (003): 328-332.

[5] Cai, Z. J., Liu, Q. (2021). Understanding the Global Cancer Statistics 2018: implications for cancer control. Science China (Life Sciences), 64 (06): 1017-1020.

[6] Wei, X., Lai, Y., Li, J. (2017). PSCA and MUC1 in non-small-cell lung cancer as targets of chimeric antigen receptor T cells. Oncoimmunology, 6 (3): e1284722.

[7] Zhang, Y. R., Zhang, T. B., Tong, D. J. Apatinib-reated gastrie cancer listing N. Science and Technology Daily. 20141108.

[8] Zhang, H. J. (2015). Apatinib for molecular targeted therapy in tumor. Drug Des Devel Ther, 9, 6075-6081.

[9] Jia, J. H., Wang, J., Gao, P. (2019). Short term efficacy and prognosis of apatinib in the treatment of metastatic colorectal cancer with chemotherapy failure. Chinese Clinical Oncology, 46 (15): 785-789.

[10] Hu, X. C., Cao, J., Hu, W. W. (2014). Multicenter phase II study of Apatinib in nontriple-negative metastatic breast cancer. BMC Cancer, 14 (1): 820.

[11] Zhang, L., Shi, M. Q., Huang, C. (2012). A phase II, multicenter, placebo-controlled trial of apatinib in patients with advanced nonsquamous non-small cell lung cancer (NSCLC) after two previous treatment regimens. J ClinOncol, 30 (15): 7548-7548.

[12] Li, X, Zhang, C. C., Tan, H. Y. (2016). Clinical effect of apatinib mesylate tablets in the treatment of advanced non-small cell lung cancer. Chinese Journal of biochemical medicine, 36 (2): 91-93.

[13] Fang, S. C., Zhang, H. T., Zhang, Y. M. (2017). Apatinib as post secondline therapy in EGFR wild-type and Alk-negative advanced lung adenocarcinoma. Onco Targets Ther, 18 (10): 447-452.

[14] Zhao, M. F. (2015). One case of advanced non-small cell lung cancer treated with apatinib. China Medical News, 30 (16): 18.

[15] Peter, L. F., Steve, H. (2008). WGCNA: an R package for weighted correlation network analysis. 9 (2): 1-32.

[16] Kuang HF, Hu YL. (2018) Mining prostate cancer development related genes with different levels of prostate specific antigen based on co expression network. Journal of Snake, 30 (02): 172-175.

[17] Qi GQ, Kong W, Mou XY, Wang SQ. (2019). A new method for excavating feature lncRNA in lung adenocarcinoma based on pathway crosstalk analysis. Journal of Cellular Biochemistry, 120 (6): 9034-9046.

[18] An Y, Zhang Q, Li X. (2018). Upregulated microRNA miR-21 promotes the progression of lung adenocarcinoma through inhibition of KIBRA and the Hippo signaling pathway. Biomedicine & Pharmacotherapy, 108, 1845-1855.

[19] Wilhite, S. E., Barrett, T. (2012). Strategies to Explore Functional Genomics Data Sets in NCBI's GEO Database. Methods in Molecular Biology, 802: 41.

[20] Zhou WX, Wang TX, Chen XR. (2016). Network analysis technology in network pharmacology. Journal of International Pharmaceutical Research, 43 (03): 399-409.

[21] Wu LH, Wang Y, Fang XH. (2011). Network pharmacology technology tools: network visualization and network analysis. China Journal of Chinese Materia Medica, 36 (21): 2923-2925.

[22] Li JH, Hu A, Zheng WJ, Hua ZC. (2014). Screening of target protein of triptolide on psoriasis by molecular docking. Chin Pharm J, 49 (13): 1133-1138.

[23] Strachan, R. T., Ferrara, G., Roth, B. L. (2006) Screening the receptorome: An efficient approach for drug discovery and target validation. Drug Discovery Today, 11 (1516): 708-716.

[24] Morris, G. M., Huey, R., Lindstrom, W. (2009). Autodock4 and AutoDockTools4: Automated docking with selective receptor flexibility. Journal of computational chemistry, 30 (16): 2785-2791.

[25] Li HJ, LiY, Hao HS. (2012). Relationship between epidermal growth factor receptor and lung development. Hereditas, (01): 27-32.

[26] Kim, J., Yoo, C., Moon, J. H., Um, S. H. (2020) EGFR Fragmentation for Topological Transformation Nanobarcoding. Chembiochem: a European journal of chemical biology, 21 (17): 2533-2539.

[27] Chen, E. H., Chen, Z. C., Chen, M. L., & Che, M. Y. (2017). Clinical effect evaluation of apatinib mesylate tablets in the treatment of advanced non-small cell lung cancer. China Modern Medicine.

[28] Yw, A., Pt, B., Lei, X. C., Li, L. A., Rui, H. A., & Mz, A. (2020). The clinical efficacy of combinatorial therapy of egfr-tki and crizotinib in overcoming MET amplification-mediated resistance from prior EGFR-TKI therapy-sciencedirect. Lung Cancer, 146, 165-173.

[29] Li, F., Zhu, T., Cao, B., Wang, J., & Liang, L. (2017). Apatinib enhances antitumour activity of egfr-tkis in non-small cell lung cancer with egfr-tki resistance. European Journal of Cancer, 84, 184-192.

[30] Peng, Y., Cui, H., Liu, Z., Liu, D., Liu, F., & Song, Y. (2017). Apatinib to combat EGFR-TKI resistance in an advanced non-small cell lung cancer patient with unknown egfr status: a case report. Oncotargets & Therapy, 10, 2289-2295.

[31] Lin, C., Wang, S. S, Xie W. W.,... & Chang J. H. (2016). Apatinib inhibits cellular invasion and migration by fusion kinase KIF5B-RET via suppressing RET/Src signaling pathway. Oncotarget, 7 (37): 59236-59244.

[32] Zhang, Q., Yu, Z. C., Bo, L., Zhang, H. M. (2019). The mechanism of apatinib on the proliferation and apoptosis of human hepatoma cells. Progress in Modern Biomedicine, 19 (13): 2424-2428.

[33] Yang, J. M., Li, J. L. (2020). Effects of apatinib mesylate on proliferation, apoptosis and PI3K / Akt signaling pathway in human colon cancer HCT-116 cells. Hebei Medical Journal, 42 (02): 212-215.

[34] Liu, Z. L., Jin, B. J., Cheng, C. G., Zhang, F. X., Wang, S. W., & Wang, Y., et al. (2017). Apatinib resensitizes cisplatin-resistant non-small cell lung carcinoma A549 cell through reversing multidrug resistance and suppressing ERK signaling pathway. European Review for Medical & Pharmacological Sciences, 21 (23): 5370.

[35] Lee, H. J., Lee, E. K., Seo, Y. E. (2017). Roles of Beh2 and CASP9 and-3 in Cix30-induced human eosinophil apopto-sis. Microbiol Immunol Infect, 50 (2): 145-152.

[36] Fornari, F., Utri, D., Patrizi, C. (2017). In Hepatocellular Carcinoma MIR 221 Modulates Sorafenib Resistance through Inhibition of CASP3 Mediated Apoptosis. Clin Cancer Res, 23 (14): 3953-3965.

[37] Wang, X. S., Uok, J., Bella, A. E. (2014). CASP 3 expression in metastatic lymph nodes of esophageal squamous cell carcinoma is prognostic of vival. World J Gastroenterol, 20 (15): 4414-4420.

[38] Chui, T. L., Su, C. C. (2017). Tanshinone II A increases proteinexpression levels of PERK, ATF6, IRELA, CHOP CASP 3 and CASP12 in pancreatic cancer BXPC-3 cell derived xenograft tumors. Mol Med Rep, 15 (5): 3259-3263.

[39] Mou, Z., Xu, X., Dong, M., Xu, J. (2016). MICRORNA-148B acts as a tumor suppressor in cervical cancer by Inducing gi/sphase cell cycle arrest and apoptosis in a CASP 3-dependent manner. Med Sci Monit, 22: 2809-2815.

[40] Huang, K., Cui, G. H., Zhao, S. (2012). Expression and relationship of BAG-1 and CASP 3 genes in non-small cell lung cancer. Chinese Journal of Gerontology, 32 (04): 696-697.

[41] Xiao, L. N., Zhou, X. R., Zhang, Q. H. (2019). Expression of CASP 3 protein in non-small cell lung cancer and its relationship with tumor cell apoptosis. Laboratory Medicine and Clinic, 16 (14): 2034-2036+2041.

[42] Liu, T. L., Wang, B., Zhao, J. J. (2010). Expression and significance of agglomeratin and CASP 3 in non-small cell lung cancer. Chinese Clinical Oncology, 15 (08): 712-716.

[43] Marx V. (2013). Tracking metast asisand tricking cancer. Nature, 494 (7435): 13-6.

[44] Shibasaki, K., & Rahman, A. (2013). Auxin and Temperature Stress: Molecular and Cellular Perspectives.

[45] Tian, Wen, Yong, S., Zhang, Jing, H., & Ji, J. (2018). Comprehensive Analysis of DNA Methylation and Gene Expression Datasets Identified MMP9 and TWIST1 as Important Pathogenic Genes of Lung Adenocarcinoma. DNA AND CELL BIOLOGY.

[46] Dorenkamp, M., Jrg P. Müller, Shanmuganathan, K. S., Schulten, H., N Müller, & Lffler, I. (2018). Hyperglycaemia-induced methylglyoxal accumulation potentiates VEGF resistance of diabetic monocytes through the aberrant activation of tyrosine phosphatase SHP-2/SRC kinase signalling axis. Scientific Reports, 8 (1): 14684-95.

[47] Yao, Xiao, J., Xun, Wang, Fu, Q., & Meng. (2017). Inhibition of invasion by N-trans-feruloyloctopamine via AKT, p38MAPK O crossMark and EMT related signals in hepatocellular carcinoma cells. Bioorganic and Medicinal Chemistry Letters, 27 (4): 989-993.

[48] Zhang, Y. M., & Zhang, L. Y. (2019). Knockdown of LASP2 inhibits the proliferation, migration, and invasion of cervical cancer cells. Journal of Cellular Biochemistry, 120 (9): 15389-15396.

[49] Sorgen, P. L., Duffy, H. S., Sahoo, P., Coombs, W., Delmar, M. & Spray, D. C. (2004). Structural Changes in the Carboxyl Terminus of the Gap Junction Protein Connexin43 Indicates Signaling between Binding Domains for c-Src and Zonula Occludens-1. Journal of Biological Chemistry. 279 (52): 54695-701.

[50] Zhen, R., Qin, X. S., Sei, J. Y. (2006). Effect of inhibition of SRC tyrosine kinase on proliferation of non-small cell lung cancer cells. Chinese Journal of Cancer Prevention and Treatment, 11 (1): 826-30.

[51] Tobias, B., Hendrik, L., Frank, G. & Hendrik, U. (2012). The Src family kinase inhibitors PP2 and PP1 effectively block TGF-beta1-induced cell migration and invasion in both established and primary carcinoma cells. Cancer Chemotherapy and Pharmacology. 34 (6): 175-6.

[52] Ruan, Y., Gong, H., Li, Y. W., Zhang, H. B., Li, Y. (2019). Effect of apatinib on invasion and migration of lung cancer cells and its mechanism. Chinese Journal of Lung Cancer, 22 (05): 16-22.

[53] Yang, S. H., Sharrocks, A. D., Whitmarsh, A. J. (2013). MAP kinase signalling cascades and transcriptional regulation. Gene, 513 (1): 3-21.

[54] Kim, E. K., Choi, E. J. (2015) Compromised MAPK signaling in human diseases: an update. Archives of Toxicology, 89 (6): 867-882.

[55] Morikawa, T., Baba, Y., Yamauchi, M.,... & Ogino, S. J. (2011). STAT3 expression, molecular features, inflammation patterns, and prognosis in a database of 724 colorectal cancers.. Clinical cancer research: an official journal of the American Association for Cancer Research. 17 (6): 1452-1462.

[56] Geiger, J. L., Grandis, J. R., Bauman, J. E. (2016). The STAT3 pathway as a therapeutic target in head and neck cancer: Barriers and innovations. Oral Oncology, 56: 84-92.

[57] Liu, A. G, Liu, Y., Jin, Z. G.,... & Jiayuh Lin. (2017). XZH-5 inhibits STAT3 phosphorylation and enhances the cytotoxicity of chemotherapeutic drugs in human breast and pancreatic cancer cells. PLoS ONE, 7 (10): e46624.

[58] Hu, C., Zhuang, W., Qiao, Y., Liu, B., Liu, L., & Hui, K., et al. (2019). Effects of combined inhibition of STAT3 and WEGFR2 pathways on the radiosensitivity of non-small-cell lung cancer cells. OncoTargets and Therapy, Volume 12, 933-944.